ACS APPLIED MATERIALS & INTERFACES

Research Article

www.acsami.org

Effective Blockage of the Interfacial Recombination Process at TiO_2 Nanowire Array Electrodes in Dye-Sensitized Solar Cells

Dianlu Jiang,[‡,†] Yuanqiang Hao,[‡,§,†] Rujuan Shen,[∥] Sevak Ghazarian,[‡] Angela Ramos,[‡] and Feimeng Zhou*[,‡]

[‡]Department of Chemistry and Biochemistry, California State University, Los Angeles, Los Angeles, California 90032

[§]College of Chemistry and Chemical Engineering, Central South University, Changsha, Hunan 410083, China

[∥]State Key Laboratory of Powder Metallurgy, Central South University, Changsha, Hunan 410083, China

Supporting Information

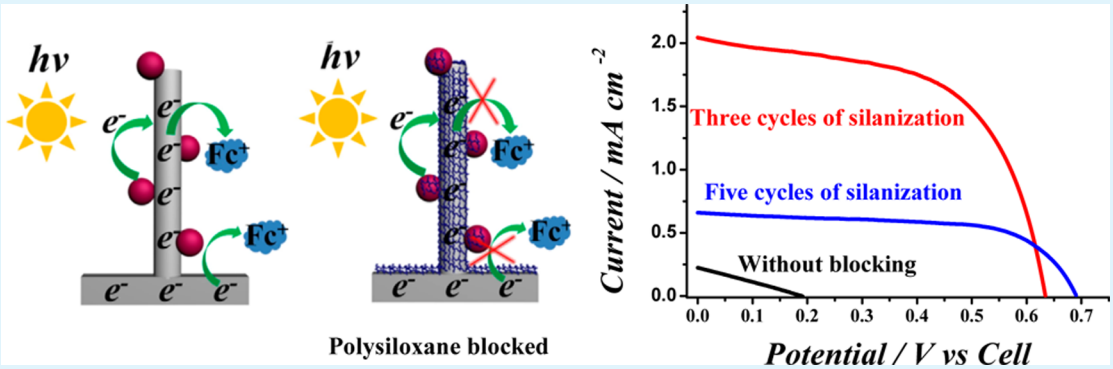

ABSTRACT: Effective blockage of recombination electron transfer of a fast electron transfer redox couple (ferrocenium/ferrocene or Fc^+/Fc) at TiO_2 nanowire array electrodes is achieved by silanization of the dye loaded TiO_2 nanowire array. FT-IR clearly shows the formation of polysiloxane network at fluorine doped tin electrodes covered with TiO_2 nanowire arrays and the dye molecules. Compared to the commonly used TiO_2 nanoparticle film electrodes, the TiO_2 nanowire array has a more spatially accessible structure, facilitating the formation of uniform polysiloxane films. Energy-dispersive X-ray spectroscopy (EDS) also reveals the presence of Si over multiple spots at the cross sections of the silanized TiO_2 nanowire array electrodes. As a result, a rather high open-cell voltage V_{oc} (0.69 V) and an enhanced efficiency (0.749 %) for DSSC with the Fc^+/Fc couple were obtained. Contrary to the passivated TiO_2 nanoparticle film electrodes at which a complex, biphasic dependence of electron lifetime on V_{oc} was observed, we recorded a logarithm linear dependence of the lifetime on V_{oc} after the silanization treatment. The nanowire arrays with optimal salinization treatments afford a useful surface for the study of electron recombination and photovoltaic generation in DSSCs.

KEYWORDS: *surface passivation, recombination blockage, silanization, nanowire array, ferrocene/ferrocenium, dye sensitized solar cells*

INTRODUCTION

Dye-sensitized solar cells (DSSCs), as a type of alternative, renewable energy source, have attracted a great deal of attention due to their low production cost, environmentally friendly fabrication processes, and relatively high solar energy conversion efficiency.[1] Since the seminal work by O'Regan and Grätzel in 1991,[2] many endeavors have been embarked on to improve the overall efficiency by optimizing the performances of host materials, harvesting dyes, and redox couples.[3−5] Although a high efficiency of 12.3% has been achieved in small-sized cells,[6] higher efficiencies are more difficult to attain for cells of larger scales.[7]

The overall solar energy-to-electricity conversion efficiency (η) in a solar cell is given by the photocurrent density measured at short-circuit (J_{sc}), the open−circuit photovoltage (V_{oc}), the fill factor of the cell (FF), and the intensity of the incident light (P_{in}).

$$\eta = \frac{J_{sc} \times V_{oc} \times \mathrm{FF}}{P_{in}} \quad (1)$$

J_{sc} can be obtained from the monochromatic, incident photon-to-current conversion efficiency (IPCE) spectrum. The IPCE of the state-of-art DSSCs exceeds 80% in the dye absorption spectrum.[6] Considering the estimated 15% loss of photons at the conducting glass electrode that supports the

Received: August 26, 2013
Accepted: November 5, 2013
Published: November 5, 2013

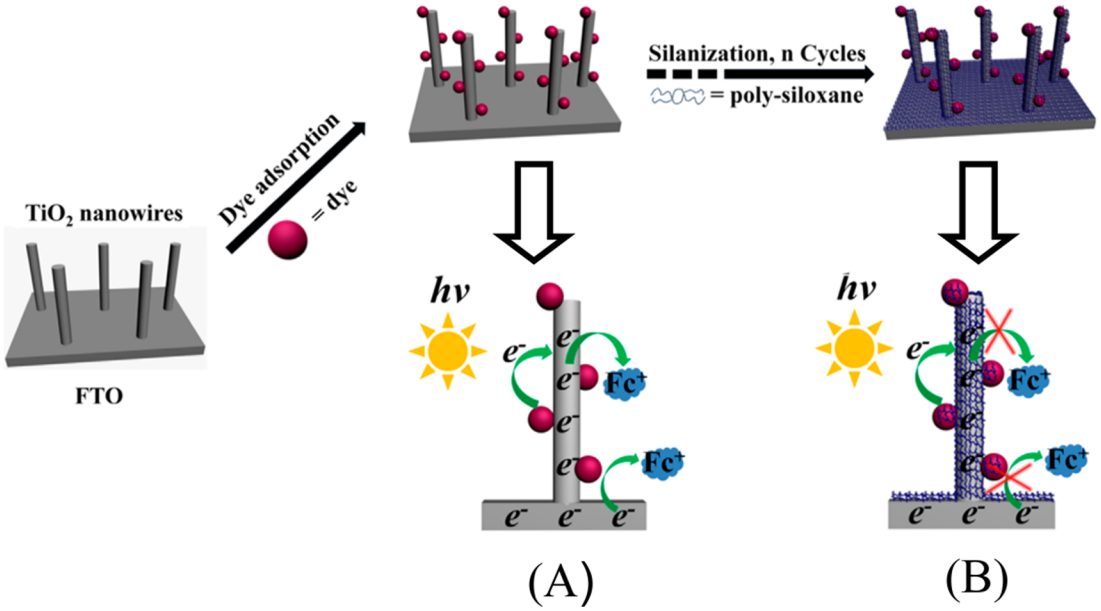

Figure 1. A schematic illustrating the recombination process at untreated dye-loaded TiO_2 nanowire arrays (enlarged view A) and the blockage of the recombination process at silanized arrays (enlarged view B).

semiconductor framework, there is little room to further increase the photocurrent in these DSSCs.[8]

Theoretically, V_{oc} is determined by the difference between the quasi-Fermi level of the TiO_2 electrode (E_f) and the potential of the redox couple ($E^{o}_{R^+/R}$), as given by eq 2.

$$V_{oc} = E_f - E^{o}_{(R^+/R)} \quad (2)$$

The mismatch in the energy between the redox potential of a given redox couple and the HOMO level of a dye sensitizer lowers the open-circuit voltage and consequently the conversion efficiency of the DSSC. The redox potential of the most effective and thus commonly used triiodide/iodide (I_3^-/I^-) redox shuttle is about 0.35 V, which is 0.77 V below the HOMO level of the standard sensitizer N719, cis-bis-(isothiocyanato)bis(2,2′-bipyridyl-4,4′-dicarboxylato)-ruthenium(II).[9] The mismatch of 0.77 V is the major loss of energy in the most advanced DSSCs. If V_{oc} could be augmented by 0.4 V, the DSSC efficiency would increase by more than 50%. Replacement of the I^-/I_3^- redox couple with one that better matches the energetics is therefore expected to improve the overall efficiency. Metal complexes containing metal centers of Co(II/III),[10,11] Fe(II/III),[12,13] and Ni(III/IV)[14,15] have been investigated on the basis that their redox potentials can be readily tuned with various ligands.[9,16,17] Despite their better match in energetics, only limited success was achieved when organic dyes were used for light absorption. Up to now no reported redox couples have shown the remarkable characteristics of the I_3^-/I^- redox couple,[6,13,18] especially when ruthenium-based dyes are used for harvesting the sun light. Unlike I_3^- of the I_3^-/I^- redox couple, the oxidation states of these metal complexes have a fast electron transfer rate with the injected electrons at the bare fluorine doped tin oxide (FTO) sites and/or at the TiO_2 surface (cf. recombination reaction shown in eq 3).[19,20] In addition, it is also likely that the dye regeneration process by these redox couples is slow. Overall, the recombination process out-competes the dye regeneration step, resulting in a significant reduction in the photocurrent and the open-circuit voltage

$$e_{TiO_2} + R^+ \rightarrow R \quad (3)$$

It is challenging to design a redox couple that simultaneously offers a matching redox potential and a slow interfacial electron transfer rate. If the recombination electron transfer pathways are blocked, V_{oc} could be raised by using redox couples with higher potentials to increase the overall efficiency. The main recombination pathway in DSSCs includes recombination of electrons injected by excited dyes at the TiO_2 and SnO_2 substrates with the oxidized redox species.[12,19] Another recombination pathway, the backward electron flow from the electrode substrate to oxidized dye molecules, is energetically disfavored and therefore not a major concern.

A number of approaches have been explored to block the main recombination pathway in DSSCs.[21−25] For example, atomic layer deposition of insulating metal oxides such as Al_2O_3 on TiO_2 has been investigated to decrease the fast interfacial recombination rate of the ferrocenium/ferrocene redox couple.[16] Usually a compact insulating layer is deposited on films of TiO_2 nanoparticles prior to the dye adsorption step. A limitation inherent in this approach is that, while the insulating layer retards the interfacial electron transfer of the redox couple, it also impedes the electron injection from the excited dye molecules. To mitigate this problem, Gregg et al. silanized the surface of dye-coated TiO_2 nanoparticles.[19] The advantage of the silane treatment is that dye molecules are embedded in the organosilane layer. If precisely controlled, it is possible to produce a blocking layer that inhibits the interfacial electron transfer of the redox couple while maintaining the electron transfer between dye molecules and the redox couple in solution. While the concept has been demonstrated previously, the non-uniformity and variable voids among the TiO_2 particles seriously compromise the efficacy of the approach. Specifically, it is difficult for silanization agents to access the porous film comprising TiO_2 nanoparticles. Inevitably, there exit ill- and over-coated regions, leading to unpredictable interfacial electron transfer behaviors and a lower DSSC performance.[12,19] In addition, the relative slow electron transfer across the grain boundary of the TiO_2 particles provides the dye-injected

electrons more time to react with the oxidized form of the redox couple.

Herein we report on the use of silane-treated (coated) one-dimensional TiO_2 nanowire arrays for DSSCs. We show that the open and spatially accessible structure of the TiO_2 nanowire arrays is favorable for the coating with uniform polysiloxane layers. In addition, the phase continuation in TiO_2 nanowires (i.e., free of grain boundaries) facilitates the transportation of injected electrons and leaves little time for them to recombine with the oxidized form of the redox couple in solution.[26] After the dye adsorption at the TiO_2 nanowire arrays supported by the FTO substrates, silanization of the surface was performed (Figure 1). We selected the ferrocence/ferrocenium (Fc^+/Fc) redox couple, which undergoes facile out-sphere electron transfer reactions, to test the efficacy of the surface blockage/passivation. We found that a proper silane passivation treatment decreases the recombination of photoinjected electrons with Fc^+ by almost four orders of magnitude. The dependence of the electron lifetimes on the silanization cycles and open-circuit potentials was also determined.

EXPERIMENTAL SECTION

Materials and Reagents. The dye sensitizer, cis-bis-(isothiocyanato) bis(2,2′-bipyridyl-4,4′-dicarboxylato)ruthenium(II) bis-tetrabutylammonium, with the moniker of N3, was purchased from Solaronix SA (Aubonne, Switzerland) and used as received. Titanium butoxide (98%), anhydrous acetonitrile (99.9%), 1-butanol (99.9%), and chloroplatinic acid hexahydrate ($H_2PtCl_6{\cdot}6H_2O \geq 37.5\%$ as Pt) were purchased from Sigma–Aldrich (Milwaukie, WI). FTO substrates (F:SnO_2, Tec 15, 10 Ω/square) were received from Hartford Glass Company (Hartford, IN). All other chemicals were of analytical grade and obtained from Thermo Fisher Scientific Inc. (Pittsburgh, PA).

Preparation of the TiO_2 Nanowire Arrays. The TiO_2 nanowire arrays were directly grown on FTO substrates by following a reported method with some modifications.[27] In a typical synthesis, 1 mL of hydrochloric acid (37 wt %) was mixed with 10 mL of toluene. This was followed by addition of 1 mL of tetrabutyl titanate. The mixture was stirred for 5 min, and 1 mL of titanium tetrachloride (1 M intoluene) was added. The final mixture was poured in a Teflon cup inside an autoclave reactor (23 mL volume, Parr Instrument Co., Moline, IL).

The FTO substrates were cleaned by sequential sonication in acetone, 2-propanol, and ethanol, which was followed by rinsing with deionized water and drying in a nitrogen stream. Clean substrates were coated with a compact TiO_2 layer, which was produced from immersion in a 0.2 M $TiCl_4$ solution for 12 h and the subsequent annealing in air at 500 °C for 0.5 h. Each as-treated FTO substrate was placed at the bottom of a reactor filled with the precursor solution. The hydrothermal growth of nanowire array in the autoclave was conducted at 180 °C for 1 h in a furnace. The autoclave was then cooled to room temperature under a flowing stream of water. The FTO substrate with TiO_2 nanoarrays was taken out and rinsed extensively with ethanol and deionized water. Prior to dye adsorption, the TiO_2 arrays were sintered in a furnace at 450 °C for 30 min. Dye adsorption onto the TiO_2 nanowire arrays was accomplished by immersing the films in a solution containing 0.5 mM N3 in ethanol overnight. The films were then rinsed in ethanol to remove any physically adsorbed dye molecules.

Surface Passivation of the TiO_2 Nanowire Arrays. The vapor-phase silanization procedure was carried out in a home-made chamber equipped with inlet and outlet valves, which is similar to those reported by others.[12,19] A shelf was mounted above the liquid container at the bottom of the chamber for the placement of N3-loaded TiO_2 film electrodes. A long pipette for silane delivery was inserted through an opening at the top of the chamber. The chamber was purged with dry N_2 gas until a relative humidity of 10 % was reached. Upon the introduction of trichloromethylsilane (0.5 mL) through the long transfer pipette into the small container, the valves were closed, and the TiO_2 nanowire arrays were allowed to be in contact with the silane vapor for 1 h. The substrates covered with the nanowire arrays were then taken out and rinsed with 2% pyridine in acetonitrile and baked at 100 °C for 15 min. The procedure was repeated for predetermined cycles.

Physical Characterizations. A scanning electron microscope (FEI, NOVA Nano SEM230) equipped with an energy-dispersive X-ray spectroscopic (EDS) accessory (Oxford Instrument, Oxford, UK) was employed to investigate the morphologies of the TiO_2 nanowire arrays.

Solar Cell Characterizations. The DSSCs were tested with a home-made cell, by using the TiO_2 film as the working electrode and a platinum-coated FTO glass as the counter electrode.[28,29] The solution contained 0.13 M Fc, 0.013 M ferrocenium tetrafluoroborate (Fc^+), and 0.2 M tetrabutylammonium tetrafluoroborate. Freshly prepared Fc^+- and Fc-containing solutions were used for the entire work. A mask with a window area of 0.0707 cm^2 was placed on the TiO_2 side of the FTO substrates to define the active area of the cell. A 500W Xe lamp (Newport Corp., Irvine, CA) with an AM 1.5G filter was used as the light source. The light intensity was measured by a radiant power meter (Model 70260, Newport Inc.). The current-voltage curves were recorded with linear sweep voltammetry (LSV) using a DY2300 potentiostat instrument (Digi-Ivy, Austin, TX). The solar energy-to-electricity conversion efficiency was calculated with eq 1. By turning off the illumination on the DSSC that has reached the steady state and monitoring the subsequent decay of V_{oc}, electron lifetime (τ_n) can be determined. We refer to this procedure as the open-circuit voltage decay (OCVD). The τ_n value is the reciprocal of the derivative of the decay curves normalized with respect to the thermal voltage[30,31]

$$\tau_n = -\frac{k_B T}{e}\left(\frac{dV_{oc}}{dt}\right)^{-1} \quad (4)$$

where k_B is the Boltzmann constant, T is the absolute temperature, e is the electronic charge, and dV_{oc}/dt is the derivative of the transient open-circuit voltage.

RESULTS AND DISCUSSION

Characterization of TiO_2 Nanowire Arrays. Shown in Figure 2 are top- and cross-sectional views of SEM images of a typical TiO_2 nanowire array. The vertically aligned and cylindrical nanowires are highly uniform and densely packed. The wires are small but long, with an average diameter of ∼30 nm and a typical length of ∼5 μm. The hydrothermal growth of vertically oriented TiO_2 nanowire arrays on FTO via the reaction at the interface between a nonpolar solvent and a hydrophilic substrate was first reported by Grimes and co-workers and has been successfully used to by others.[27,32−34] The method produces thinner wires than aqueous solution, allowing more dye adsorption for a given array film. At low temperature, titanium precursors and water (from hydrochloric acid solution) are separated, and the precursors remain in toluene and hydrolysis occurs at the interface. Under hydrothermal conditions, a better mixing of the two different phases facilitates the precursor hydrolysis. The hydrolyzed TiO_2 moieties deposit on the crystal nuclei at the hydrophilic FTO surface, which is followed by contraction and rearrangement for further crystal growth. Hydrochloric acid is used to ensure an acidic environment and to retard hydrolysis of the precursor. The Cl^- ions play an important role in the hydrothermal growth as they promote anisotropic growth of one-dimensional nanocrystals.[27,35]

Surface Passivation and Current-Voltage Characteristics. As discussed in the Introduction, for a redox couple with a fast interfacial electron transfer rate, an electrically insulating

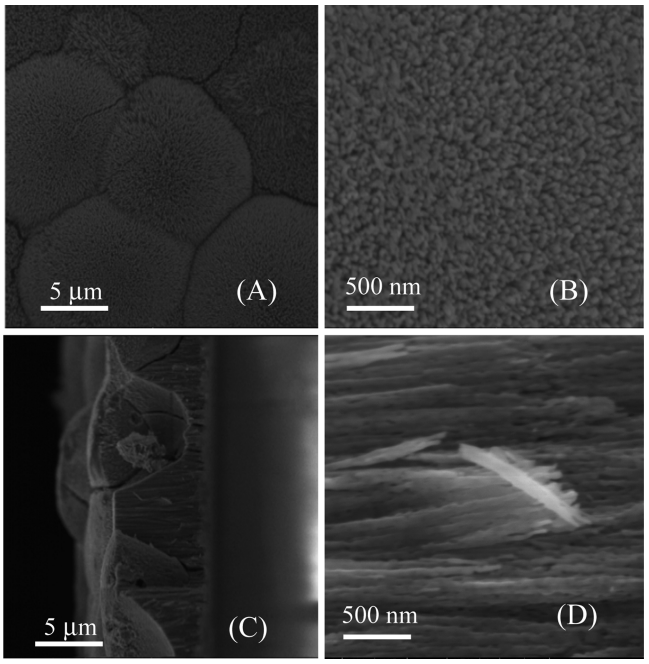

Figure 2. SEM images of vertically oriented, self-organized TiO_2 nanowire arrays grown on FTO-coated glass substrates at 180 °C for 1 h in top- (panels A and B) and cross-sectional (panels C and D) views.

layer that is sufficiently thick to prevent electron tunneling should effectively inhibit the interfacial recombination process between the oxidized form of the redox couple and the injected electrons.[12,19]

The silanization passivation process is depicted in Scheme 1. First, the trichloromethylsilane adsorbs onto the TiO_2 surface and reacts with the hydroxyl groups on the surface. The subsequently adsorbed trichloromethylsilane molecules cross-link with the preformed monolayer and polymerize in a moisturized environment. Controlling the moisture level during the silanizaton is critical to the formation of the desired thickness of the polysiloxane layer. We have investigated the impact of chamber humidity on the layer thickness by purging the chamber with N_2, rinsing the loosely adsorbed silane molecules and baking the nanowire array for various times to facilitate the crosslinking of the adsorbed silane molecules. Our results demonstrated that under low humidity (<5%) in the chamber polysiloxane layers could not be formed. This is because, without the condensation reactions shown in steps I, II, and III of Scheme 1, the silane molecules are only adsorbed loosely and would be readily washed off or evaporated away. We found that a humidity of 10% produced the best results. Figure 3 shows a representative FT-IR spectrum of a TiO_2 nanowire array after one cycle of silanization. The band at 1035 cm^{-1} is attributed to the Si−O−Si stretching in the polysiloxane network. A characteristic band at about 1274 cm^{-1} was also observed, which can be assigned to bending of the methyl

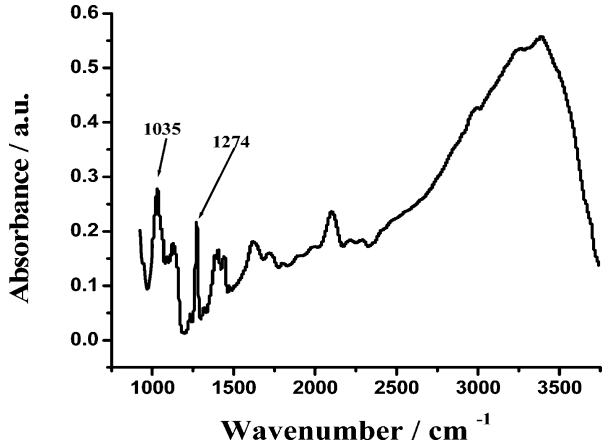

Figure 3. IR spectrum of an N3-loaded TiO_2 nanowire array after the treatment of one cycle of salinization with trichloromethylsilane.

Scheme 1. Schematic Diagram Showing the Attachment of Trichloromethylsilane to the Surface of the TiO_2 Nanowires and the Formation of a Polymerized Layer on a Hydroxyl-Terminated TiO_2 Surface

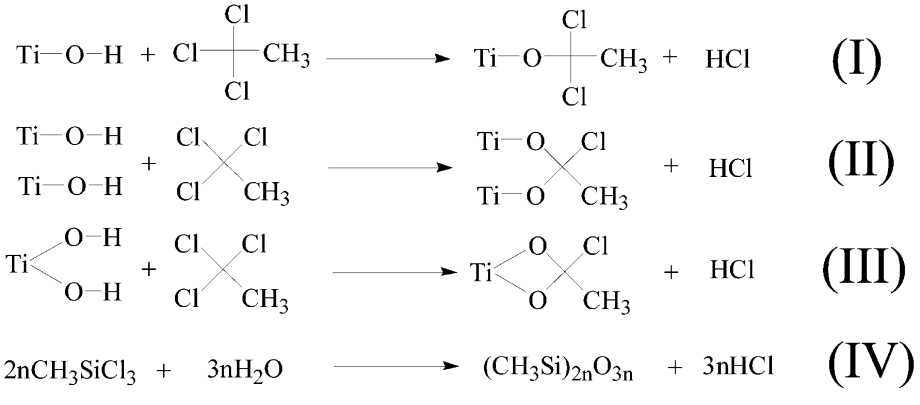

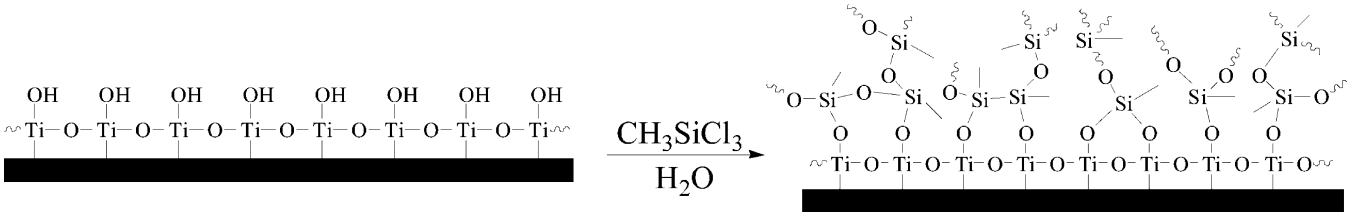

dx.doi.org/10.1021/am4036042 | ACS Appl. Mater. Interfaces 2013, 5, 11906−11912

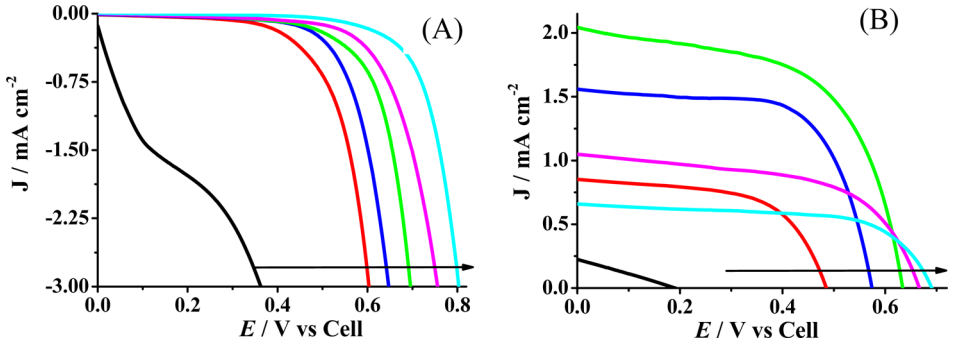

Figure 4. Current density J plotted against potential E at the TiO_2 nanowire array that had undergone 0 (black), 1 (red), 2 (blue), 3 (green), 4 (magenta), and 5 (cyan) cycles of silanization. Panel A shows the dark currents, while panel B was constructed with data collected under the illumination of light equivalent to one sun. An acetonitrile solution containing ferrocenium (0.013 mM) and ferrocene (0.13 mM) as the redox couple was used.

groups in the trichloromethylsilane molecules.[12,36−38] This is indicative of the presence of trichloromethylsilane molecules in the poly(methylsiloxane) film deposited onto the hydroxylated TiO_2 nanowires. We also conducted the elemental analysis (energy-dispersive X-ray spectroscopy or EDS) of different spots spanning the cross section of the nanowire array film that had been silanized and compared the results to those obtained at a film without silanization treatment. As shown in Table S1 (Supporting Information), at the cross section of the bare nanowire array film no Si was detected. In contrast, as shown in Table S2, at a few randomly selected spots on the cross section of a silanized nanowire array film, a comparable percentage of Si (1 %) was detected with less than 30% variation. Such a variation is not large considering that the randomly sampled spots do not cover the same amount of void space or surface areas of nanowires. The variations in the percentages of other elements from spot to spot support this contention. Overall, the relatively small variation of Si atoms across the film is indicative of the accessibility of the array film to silanization or other chemical modification.

The effectiveness in the inhibition of the recombination pathway is dependent on the thickness of and defects in the polysiloxane layer. Pinholes may exist in the layer, leading to undesired interfacial electron transfer reactions. Even for a pinhole-free monolayer of silane molecules, electron tunneling across the layer will lead to rapid recombination.[39] On the other hand, if the layer is too thick, it will be detrimental to the desired electron transfer between the dye and the redox couple. Therefore, an optimal thickness needs to be determined. Figure 4 shows the current density plotted against potential applied to the TiO_2 nanowire arrays that had undergone different cycles of silanization. As expected, the dark current at the untreated, dye-loaded TiO_2 nanowire arrays (black line curve in panel A) increases right after the potential was scanned away from 0.0 V against the counter electrode. After one cycle of silanization of the nanowire arrays, the dark current is drastically decreased (cf. the much delayed onset in panel A), and the current-voltage curves all exhibit a behavior that is characteristic of electron tunneling across a barrier.[40] Based on the current attenuation, the thickness of the silane film is much more than that of a monolayer, suggesting even one silanization cycle leads to the formation of a multilayered polysiloxane network. More silanization cycles further decrease the current or delay the onsets of the curves, indicating that the interfacial electron transfer of the redox couple was impeded to greater extents. We should note that the curves in Figure 4A are better defined than those obtained from silanized films of TiO_2 nanoparticles,[12,19] demonstrating that the blockage of the sites on the TiO_2 nanowire array with silane is more effective. We attribute such an effective blockage to the uniformity of the blocking layer resulted from the even accessibility of saline molecules to the well aligned nanowires.

Under the illumination of one sun (Figure 4B), a rather weak photovoltaic effect (black curve) was observed at an untreated TiO_2 nanowire array, with low J_{sc} (0.224 mA·cm^2) and V_{oc} (0.19 V) values. The small photocurrent decays rapidly with the applied potential, consistent with previous reported results.[12,14−16] In contrast, after silanization treatments, the J_{sc} value increased until the third cycle and began to decrease in later cycles. The decline in the J_{sc} value after the fourth and fifth cycles indicates that the polysiloxane layer has grown over some of the dye molecules and therefore hinders their electron transfer with the redox couple in solution. Interestingly, the V_{oc} value increases with the number of silanization cycles. The open-circuit voltage of the electrode continues to increase after five cycles of silanization to about 0.690 V at the expense of a substantial decrease in the short-circuit current. Although the increase in V_{oc} is substantial, it is still 0.5 V below the theoretical value. This is most likely caused by the nonuniformity of the polysiloxane layer. At sites covered with thin polysiloxane layers, electron tunneling contributes to the recombination process. Despite this, it is evident from our data that the polysiloxane (passivation) layer has drastically retarded the recombination process. It is anticipated that, for other redox couples that render more sluggish interfacial electron transfer kinetics than the Fc^+/Fc couple, the blockage of the recombination process should be even more effective. Although the overall performance is not the focus of our work, we have demonstrated the concept of utilizing the spatially accessible surface of the TiO_2 nanowire array for more effective blockage of the recombination process. In Table 1 we summarized the key parameters of the cell. The cell showed an optimal efficiency of 0.749% after three cycles of treatments, which is better than that achieved with electrodes coated with TiO_2 nanoparticles using the same redox couple.[12,19] It is worth pointing out that the value reported herein was achieved by using the nanoarray electrode with a surface area that is at least two fold smaller than electrodes covered with TiO_2 nanoparticles. The advantage would be more pronounced if a denser array with thinner and longer TiO2 nanowires was produced and used.

Table 1. Cell Parameters and Comparison to Representative Literature Values

coating cycles	J_{sc} (mA/cm^2)	V_{oc} (volt)	fill factor	efficiency (%)	refs
0	0.224	0.190	0.263	0.011	this work
1	0.852	0.486	0.587	0.243	this work
2	1.559	0.573	0.658	0.588	this work
3	2.043	0.634	0.578	0.749	this work
4	1.049	0.660	0.572	0.396	this work
5	0.660	0.690	0.634	0.289	this work
2	1.020	0.553	0.642	0.360	ref 12

Electron Lifetime. Photogenerated electrons can be injected from the excited dye molecules into the TiO_2 nanowires. There are a few paths for the electrons to flow through, which include the recombination with dye molecules and with the oxidized form of the redox couple in solution (undesired paths) and the movement through the external circuit to the counter electrode (the desired path). Under the open-circuit condition, the recombination process is the only path. So the electron lifetime reflects the recombination process. The electron lifetime (τ_n) in DSSCs derived from the OCVD measurement has been widely used as a kinetic parameter, which contains useful information on the rate constant of the electron transfer process in DSSC. In addition to evaluating the blocking efficacy based on the values of J_{sc}, V_{oc}, and η, we also measured the electron lifetimes at nanowire arrays that had been treated with different silanization cycles. Figure 5 shows the OCVD curves and the lifetime variations with the open-circuit voltage. The electron lifetime is the time during which they can be captured (intercepted) experimentally and therefore is inversely proportional to the interception rate constant. Our data show that the electron lifetime increases dramatically after silanization. After five cycles of silanization the electron lifetime increases by up to four orders of magnitude. In Figure 5A, the exponential decays of the electron lifetimes can be assigned to the tunneling of the injected electrons across the polysiloxane layer to recombine with Fc^+ in solution. The electron lifetime for the Fc^+/Fc redox couple at the nanowire array treated with five cycles is comparable to that reported for the I_3^-/I^- redox couple at an untreated film of TiO_2 nanoparticles.[41] This suggests that surface blocking should be a viable way for the use of a redox couple that is fast in electron transfer and at the same time better matches the energetics in DSSCs. Noticed from Figure 5B that, at the silanized nanowire arrays, the electron lifetime exhibits a logarithm-linear dependence on the open-circuit potential. This is indicative of a single recombination pathway. We noticed that this behavior is in contrast to that of silane-treated TiO_2 nanoparticles,[12] which display a complex, biphasic behavior containing both fast and slow components. The difference can be attributed to the spatially accessible structure of the nanowire arrays, which facilitates the formation of uniform polysiloxane layers.

CONCLUSIONS

We have demonstrated the feasibility of using a highly reversible (fast) redox couple at well aligned TiO_2 nanowire arrays for DSSC. The spatially accessible structure renders an inherent advantage for surface blockage (passivation) with organosilane molecules, whose gaseous form can readily diffuse into the voids among the nanowires. Consequently, uniform polysiloxane layers can be produced, which effectively block the recombination reaction between the injected electrons and the oxidized form of the fast redox couple (Fc^+/Fc in the present case). With a much smaller surface area, the TiO_2 nanowire array leads to a higher efficiency than the counterpart based on TiO_2 nanoparticles. To the best of our knowledge, both the open-circuit voltage (V_{oc}) and the conversion efficiency (η) in our work are the highest among DSSCs using Fc^+/Fc as the redox couple. Contrary to the siliane-treated TiO_2 nanoparticles where the injected electrons show a complex, biphasic lifetime dependence on V_{oc}, at our silanized nanowire arrays the injected electrons exhibit a single exponential dependence on V_{oc}. The varied accessibility within the film of TiO_2 nanoparticles to the silanization agent results in an uneven passivation layer and consequently yields a different interfacial behavior. It is anticipated that the application of uniformly passivated nanowire arrays to the study of facile electron transfer redox couples in DSSC will provide useful insight into the electron recombination mechanism. With a denser array of thinner and longer TiO_2 nanowires, we envision that higher conversion efficiency can be achieved and the energetics of DSSCs can be better tuned with many other facile electron transfer redox couples.

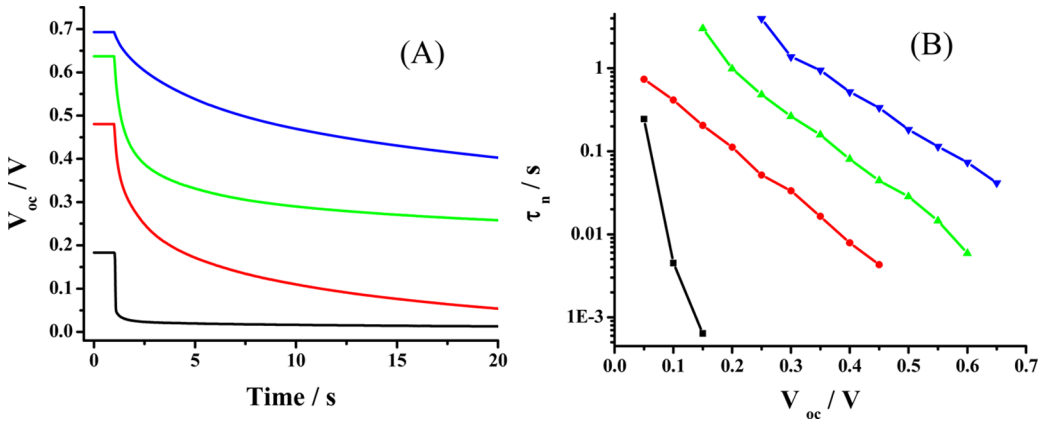

Figure 5. (A) Open-circuit voltage decay curves and (B) electron lifetimes at TiO_2 nanowire arrays treated with 0 (black), 1 (red), 3 (green), and 5 (blue) silanization cycles.

■ ASSOCIATED CONTENT

Supporting Information

EDX elemental analyses of the array film before and after silanization. This material is available free of charge via the Internet at http://pubs.acs.org.

■ AUTHOR INFORMATION

Corresponding Author

*Phone: (323) 343-2390. Fax: (323) 343-6490. E-mail: fzhou@calstatela.edu.

Author Contributions

†These authors contributed equally to this work.

Notes

The authors declare no competing financial interest.

■ ACKNOWLEDGMENTS

Partial support of this work by the National Science Foundation Center for Research Excellence in Science and Technology (NSF HRD-0932421), the ACS-Petroleum Research Funds (49390-UR10), and an NSF-RUI grant (1112105) is gratefully acknowledged.

■ REFERENCES

(1) Hagfeldt, A.; Boschloo, G.; Sun, L.; Kloo, L.; Pettersson, H. *Chem. Rev.* **2010**, *110*, 6595−6663.
(2) O'Regan, B.; Grätzel, M. *Nature* **1991**, *353*, 737−740.
(3) Roy-Mayhew, J. D.; Bozym, D. J.; Punckt, C.; Aksay, I. A. *ACS Nano* **2010**, *4*, 6203−6211.
(4) Wang, M.; Chamberland, N.; Breau, L.; Moser, J.-E.; Humphry-Baker, R.; Marsan, B.; Zakeeruddin, S. M.; Gräzel, M. *Nat. Chem.* **2010**, *2*, 385−389.
(5) Ito, S.; Murakami, T. N.; Comte, P.; Liska, P.; Grätzel, C.; Nazeeruddin, M. K.; Grätzel, M. *Thin Solid Films* **2008**, *516*, 4613−4619.
(6) Yella, A.; Lee, H.-W.; Tsao, H. N.; Yi, C.; Chandiran, A. K.; Nazeeruddin, M. K.; Diau, E. W.-G.; Yeh, C.-Y.; Zakeeruddin, S. M.; Grätzel, M. *Science* **2012**, *334*, 629−634.
(7) Sastrawan, R.; Beier, J.; Belledin, U.; Hemming, S.; Hinsch, A.; Kern, R.; Vetter, C.; Petrat, F. M.; Prodi-Schwab, A.; Lechner, P.; Hoffmann, W. *Sol. Energy Mater. Sol. Cells* **2006**, *90*, 1680−1691.
(8) Snaith, H. J. *Adv. Funct. Mater.* **2010**, *20*, 13−19.
(9) Feldt, S. M.; Wang, G.; Boschloo, G.; Hagfeldt, A. *J. Phys. Chem. C* **2011**, *115*, 21500−21507.
(10) Klahr, B. M.; Hamann, T. W. *J. Phys. Chem. C* **2009**, *113*, 14040−14045.
(11) Feldt, S. M.; Gibson, E. A.; Gabrielsson, E.; Sun, L.; Boschloo, G.; Hagfeldt, A. *J. Am. Chem. Soc.* **2010**, *132*, 16714−16724.
(12) Feldt, S. M.; Cappel, U. B.; Johansson, E. M. J.; Boschloo, G.; Hagfeldt, A. *J. Phys. Chem. C* **2010**, *114*, 10551−10558.
(13) Daeneke, T.; Kwon, T.-H.; Holmes, A. B.; Duffy, N. W.; Bach, U.; Spiccia, L. *Nat. Chem.* **2011**, *3*, 211−215.
(14) Spokoyny, A. M.; Li, T. C.; Farha, O. K.; Machan, C. W.; She, C.; Stern, C. L.; Marks, T. J.; Hupp, J. T.; Mirkin, C. A. *Angew. Chem., Int. Ed.* **2010**, *49*, 5339−5343.
(15) Li, T. C.; Spokoyny, A. M.; She, C.; Farha, O. K.; Mirkin, C. A.; Marks, T. J.; Hupp, J. T. *J. Am. Chem. Soc.* **2010**, *132*, 4580−4582.
(16) Hamann, T. W.; Farha, O. K.; Hupp, J. T. *J. Phys. Chem. C* **2008**, *112*, 19756−19764.
(17) Sapp, S. A.; Elliott, C. M.; Contado, C.; Caramori, S.; Bignozzi, C. A. *J. Am. Chem. Soc.* **2002**, *124*, 11215−11222.
(18) Kashif, M. K.; Axelson, J. C.; Duffy, N. W.; Forsyth, C. M.; Chang, C. J.; Long, J. R.; Spiccia, L.; Bach, U. *J. Am. Chem. Soc.* **2012**, *134*, 16646−16653.
(19) Gregg, B. A.; Pichot, F.; Ferrere, S.; Fields, C. L. *J. Phys. Chem. B* **2001**, *105*, 1422−1429.
(20) Wang, H.; Nicholson, P. G.; Peter, L.; Zakeeruddin, S. M.; Grätzel, M. *J. Phys. Chem. C* **2010**, *114*, 14300−14306.
(21) Wang, Z.-S.; Yanagida, M.; Sayama, K.; Sugihara, H. *Chem. Mater.* **2006**, *18*, 2912−2916.
(22) Shin, Y.-J.; Lee, J.-H.; Park, J.-H.; Park, N.-G. *Chem. Lett.* **2007**, *36*, 1506−1507.
(23) Palomares, E.; Clifford, J. N.; Haque, S. A.; Lutz, T.; Durrant, J. R. *J. Am. Chem. Soc.* **2002**, *125*, 475−482.
(24) Liu, W.; Kou, D.; Cai, M.; Hu, L.; Sheng, J.; Tian, H.; Jiang, N.; Dai, S. *J. Phys. Chem. C* **2010**, *114*, 9965−9969.
(25) Li, T. C.; Góes, M. S.; Fabregat-Santiago, F.; Bisquert, J.; Bueno, P. R.; Prasittichai, C.; Hupp, J. T.; Marks, T. J. *J. Phys. Chem. C* **2009**, *113*, 18385−18390.
(26) Feng, X.; Zhu, K.; Frank, A. J.; Grimes, C. A.; Mallouk, T. E. *Angew. Chem., Int. Ed.* **2012**, *51*, 2727−2730.
(27) Feng, X.; Shankar, K.; Varghese, O. K.; Paulose, M.; Latempa, T. J.; Grimes, C. A. *Nano Lett.* **2008**, *8*, 3781−3786.
(28) Jin, W.-M.; Shin, J.-H.; Cho, C.-Y.; Kang, J.-H.; Park, J. H.; Moon, J. H. *ACS Appl. Mater. Inter.* **2010**, *2*, 2970−2973.
(29) Trupke, T.; Baumgärtner, S.; Würfel, P. *J. Phys. Chem. B* **1999**, *104*, 308−312.
(30) Zaban, A.; Greenshtein, M.; Bisquert, J. *ChemPhysChem* **2003**, *4*, 859−864.
(31) Yu, H.; Zhang, S.; Zhao, H.; Will, G.; Liu, P. *Electrochim. Acta* **2009**, *54*, 1319−1324.
(32) Feng, X.; Shankar, K.; Paulose, M.; Grimes, C. A. *Angew. Chem., Int. Ed.* **2009**, *121*, 8239−8242.
(33) Hoang, S.; Guo, S.; Mullins, C. B. *J. Phys. Chem. C* **2012**, *116*, 23283−23290.
(34) Hoang, S.; Guo, S.; Hahn, N. T.; Bard, A. J.; Mullins, C. B. *Nano Lett.* **2012**, *12*, 26−32.
(35) Liu, B.; Aydil, E. S. *J. Am. Chem. Soc.* **2009**, *131*, 3985−3990.
(36) Tripp, C. P.; Hair, M. L. *Langmuir* **1991**, *7*, 923−927.
(37) Tripp, C. P.; Hair, M. L. *J. Phys. Chem.* **1993**, *97*, 5693−5698.
(38) Tripp, C. P.; Kazmaier, P.; Hair, M. L. *Langmuir* **1996**, *12*, 6407−6409.
(39) Barbara, P. F.; Meyer, T. J.; Ratner, M. A. *J. Phys. Chem.* **1996**, *100*, 13148−13168.
(40) Selzer, Y.; Salomon, A.; Cahen, D. *J. Phys. Chem. B* **2002**, *106*, 10432−10439.
(41) Boschloo, G.; Häggman, L.; Hagfeldt, A. *J. Phys. Chem. B* **2006**, *110*, 13144−13150.